

SCALING PROPERTIES OF NUCLEAR GIANT RESONANCE TRANSITION PROBABILITIES

A.Z. GÓRSKI AND S. DROŹDŹ

Institute of Nuclear Physics
Radzikowskiego 152, 31-342 Kraków, Poland
e-mail: gorski@alf.ifj.edu.pl

(Received September 9, 1996)

Multifractal scaling analysis of nuclear giant resonance transition probability distributions is performed within the approximation which takes into account the one-particle-one-hole ($1p-1h$) and $2p-2h$ states. A new measure to determine the fractal dimensions of the spectra is introduced. It is found that chaotic dynamics governing the decay leads to non-trivial multifractal scaling properties. Such a kind of scaling is absent in the case of regular dynamics. The degree of collectivity is another element which worsens the scaling.

PACS numbers: 05.45.+b, 24.60.Lz, 24.30.Cz

1. Introduction

There exist well established methods to identify chaotic behaviour in classical non-linear dynamical systems. It is, however, not fully clear what are the signatures of chaoticity at the quantum level. In fact, several indicators have been suggested. For systems with complex energy spectra the statistical analysis of their fluctuations has been introduced by Wigner in the context of compound nuclei. The Wigner form of the nearest neighbor spacing (NNS) distribution turns out to be a good indication that an underlying classical system is chaotic. This distribution can be simulated within the random matrix theory by the Gaussian orthogonal ensemble (GOE), while the spectra of regular systems have Poissonian distribution [1, 2]. The NNS test can be successfully applied to stationary systems and the information about the energy spectrum is sufficient. However, one would be interested to take into account more information included in the wave function [3]. The aim of this research is to find further signatures of chaos coming from the structure of the wave functions. In particular, chaotic dynamics on the classical level is known to be associated with various fractal structures obeying

the scaling relations [4]. It would be extremely interesting to identify a trace of such structures also on the quantum level.

To this end we shall consider the nuclear giant resonances as physically interesting excitations and we shall investigate their energy spectra and the transition probabilities resulting from the coupling to more complex configurations. These quantities are in principle measurable experimentally thus our predictions are verifiable. In particular, our calculations have been done for the ^{40}Ca nucleus and its $J^\pi = 2^+$ excitations to have the well defined angular momentum and parity quantum numbers. The centroid energies of nuclear giant resonances are relatively well described within the mean field 1-particle-1-hole (1p-1h) approximation. To describe its decay one needs to include states of the np - nh type. Truncating on the $2p$ - $2h$ level is, however, technically necessary (to have the hamiltonian matrix of a manageable size) and physically well justified [5]. As the nuclear forces are predominantly two-body in nature an initially excited giant resonance (a superposition of the 1p-1h states) can couple directly to the $2p$ - $2h$ states only [6]. In particular, within this approximation one obtains a good agreement with experimental data. Furthermore, the corresponding spectral fluctuations fulfill the GOE characteristics [7] which implies an underlying chaotic dynamics and the fact that already the subspace of the $2p$ - $2h$ states properly simulates relevant characteristics of the compound nuclei [8].

2. The physical model

The general form of the Hamiltonian in our model reads:

$$\hat{H} = \sum_i \varepsilon_i a_i^\dagger a_i + \frac{1}{2} \sum_{ij,kl} v_{ij,kl} a_i^\dagger a_j^\dagger a_l a_k, \quad (1)$$

where the first term (H_0) is the mean field part and the second term (V) is the residual interaction. For calculations we specify H_0 in terms of a local Woods-Saxon potential including the Coulomb interaction. The interaction part, V , was taken as the zero range Landau-Migdal interaction with the empirical parameters taken from [9].

The Hilbert space in our model is spanned by the 1p-1h and 2p-2h vectors defined in terms of the creation and annihilation operators:

$$|1\rangle \equiv a_p^\dagger a_h |0\rangle, \quad |2\rangle \equiv a_{p_1}^\dagger a_{p_2}^\dagger a_{h_2} a_{h_1} |0\rangle, \quad (2)$$

such that they diagonalize the operator H_0 in 1p-1h and 2p-2h sectors and $\langle 1|H_0|2\rangle = 0$.

We prediagonalize the Hamiltonian \hat{H} in the two sectors separately by changing the basis as follows:

$$|\tilde{1}\rangle \equiv \sum_1 C_1^{\tilde{1}} |1\rangle, \quad |\tilde{2}\rangle \equiv \sum_2 C_2^{\tilde{2}} |2\rangle. \quad (3)$$

The Schrödinger equation then reads:

$$\begin{bmatrix} E_{\tilde{1}} & A_{\tilde{1}\tilde{2}} \\ A_{\tilde{1}\tilde{2}}^* & E_{\tilde{2}} \end{bmatrix} \begin{bmatrix} X_{\tilde{1}} \\ X_{\tilde{2}} \end{bmatrix} = E \begin{bmatrix} X_{\tilde{1}} \\ X_{\tilde{2}} \end{bmatrix}, \quad (4)$$

where $E_{\tilde{1},\tilde{2}}$ are diagonal block-matrices, $A_{\tilde{1}\tilde{2}}, A_{\tilde{2}\tilde{1}}^*$ are the off-diagonal blocks and

$$A_{\tilde{1}\tilde{2}} = \sum_{12} C_1^{\tilde{1}} \langle 1|v|2\rangle C_2^{\tilde{2}}. \quad (5)$$

The A blocks are responsible for the coupling between these two sectors and 'leaking' of the probability from the $1p-1h$ sector to the $2p-2h$ one.

We consider two distinct and physically interesting cases:

- A) No residual interaction in the subspace spanned by $|2\rangle$ ($V = 0$ in that subspace). In this case the only non-vanishing matrix elements of the type $\langle 2|\hat{H}|2'\rangle$ are the diagonal ones ($\langle 2|\hat{H}|2'\rangle = \langle 2|\hat{H}_0|2'\rangle = \varepsilon_2 \delta_{22'}$). The fluctuation properties of ε_2 are then those characteristic for the regular systems [5].
- B) All the matrix elements are included which results in the GOE fluctuations of the energy spectra ε_2 typical for classically chaotic systems [5].

By comparing these two versions of our model one can then study the influence of chaotic dynamics on quantum decay.

The transition probabilities that will be used in the following Section to define our measure (11) are taken as transitions between the ground state ($|0\rangle$) and the excited states ($|i\rangle$) enumerated by $i = 1, 2, \dots, N$. In our notation a state $|i\rangle$ can be expressed as a superposition of states from both sectors:

$$|i\rangle = \sum_1 a_1^i |1\rangle + \sum_2 a_2^i |2\rangle, \quad (6)$$

and the quadruple transition operator reads:

$$\hat{O} = \hat{Q} Y_2(\theta) r^2, \quad (7)$$

where \hat{Q} is the standard charge operator: $\hat{Q} = \frac{1}{2}(1 + \tau_3)$, τ_3 being the (isospin) Pauli matrix. The first term in \hat{Q} defines the isoscalar and the second term the isovector component of the transition.

The transition probabilities can be computed directly from the following formula:

$$\rho_i = |\langle 0 | \hat{O} | i \rangle|^2. \quad (8)$$

Since the transition operator defined by Eq. (7) is one-body in nature it picks-up the $1p-1h$ components of $|i\rangle$ only and thus:

$$\rho_i = \left| \sum_{\bar{1}1} X_{\bar{1}} C_1^{\bar{1}} \langle 0 | \hat{O} | 1 \rangle \right|^2. \quad (9)$$

In principle, any state $|i\rangle$ includes certain admixture of $|1\rangle$ and, therefore, an originally (with no coupling to $|2\rangle$) localized transition strength becomes much more fragmented.

To have good quantum numbers we take the ^{40}Ca nucleus with the angular momentum and parity: $J^\pi = 2^+$. Taking into account four mean field nuclear shells (two shells above and two below the Fermi surface) this implies 26 $1p-1h$ states and 3 014 $2p-2h$ states. Here, the centroid energy is 31 and 25 MeV for isovector and isoscalar transitions respectively, with dispersion of the order of 5 MeV. Figs. 1 and 2 display the transition probabilities for different energy levels in the regular (a) and chaotic case (b) for isovector and isoscalar transitions, respectively. Even at this level one can observe a clear distinction between regular and chaotic cases. The later case even suggests a certain kind of self-similarity regarding the clustering and the relative size of the transitions. For this reason the following Section is an attempt to perform a more systematic analysis of these transition probabilities in the spirit of the Renyi exponents [10].

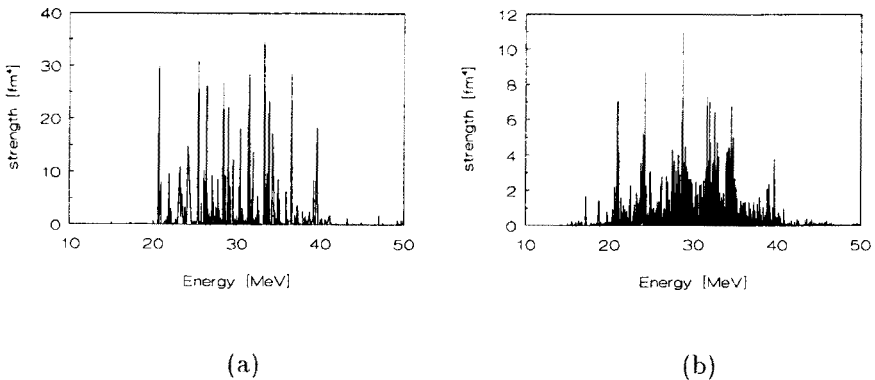


Fig. 1. Isovector quadrupole strength distribution in our model ^{40}Ca nucleus for the regular (a) and the chaotic (b) case. Note different scales.

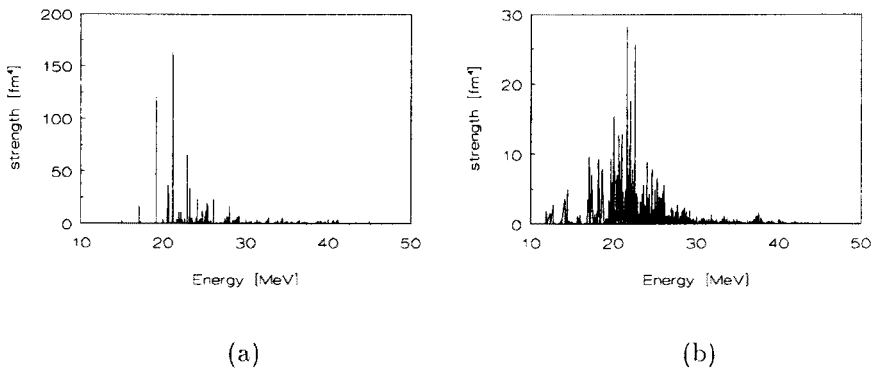


Fig. 2. The same as Fig. 1 for the isoscalar strength distribution.

3. Scaling analysis

The standard definition of a measure to compute the fractal (Renyi) dimensions (exponents) for a set of n points in N boxes (intervals) of a size l is:

$$p_i(l) = \frac{n_i}{n} , \quad (10)$$

where $n_i = n_i(l)$ denotes number of points in the i -th box (interval) and the measure is properly normalized due to: $\sum_i n_i = n$. With this measure one can determine the fractal dimensions d_q (q being any real number) by taking the limit $l \rightarrow 0$ and extracting the exponent from the following formula [11]:

$$\sum_i p_i^q(l) \sim l^{(q-1)d_q} \quad (l \rightarrow 0) , \quad (11)$$

where the log-log plot of the left hand side of Eq. (11) *vs* N is used to compute the standard scaling exponents d_q .

Applying these ideas to our energy levels only we get not a very interesting result as the energy spectrum of a typical quantum systems has dimension equal to one and the same holds true in both our cases. (There exist however systems whose energy spectra display a fractal character [12].) Therefore, consistently with our previous discussion we are going to consider the sets of *pairs* of points, the i -th pair containing two numbers: the energy and the transition probability, $\{E_i, \rho_i\}$. Taking into account the probabilities ρ_i we have a more complicated structure. Because to each energy corresponds exactly one probability the whole structure is expected to have dimension in the range $[0, 1]$ if the idea of scaling applies. Of course, due

to non-uniformity of the probability distributions the dimensions should depend on q [13].

The specific value of ρ_i can be interpreted as a frequency with which the energy $\{E_i\}$ is 'visited' and this modifies an effective number of energy levels in a given box. In this way each energy point gets a different weight. To have a measure with the proper normalization we define, instead of (10), the following new measure $P_i(l)$:

$$P_i(l) \equiv \left[\sum_{\text{all}} \rho_i \right]^{-1} \times \sum_{E_i \in i\text{-th box}} \rho_i, \quad (12)$$

where the summation in the numerator goes over probabilities whose energies are included in the i -th box. Here again the measure $P_i(l)$ is properly normalized: $\sum_i P_i(l) = 1$. The scaling exponent ("fractal dimension") with the measure (12) we will denote by D_q , while d_q we reserve for the standard fractal dimension. From (12) it is clear that in the limit $q \rightarrow 0$ (capacity dimension) the different nonzero probabilities ρ_i give the same contribution to the left hand side of (11), because the measure $P_i(l)$ is in the power of 0:

$$\lim_{q \rightarrow 0} P_i^q(l) = \lim_{q \rightarrow 0} p_i^q(l) = \begin{cases} 1 & \text{if } i\text{-th box is not empty,} \\ 0 & \text{if } i\text{-th box is empty.} \end{cases} \quad (13)$$

Hence, we have: $D_0 = d_0$, the last being the standard capacity dimension. In general, both measures and the corresponding dimensions differ for $q > 0$ according to: $0 \leq D_q \leq d_q$. The differences reflect a degree of non-uniformity in the probability distribution. To determine the scaling exponents we use the formula (11) with the new measure (12):

$$x_q(l) \equiv \sum_i P_i^q(l) \sim l^{(q-1)D_q} \quad (l \rightarrow 0), \quad (14)$$

and the log-log plot of the quantity $x_q(l)$ of Eq. (14) vs the number of boxes N is used to extract the scaling exponents D_q in Figs. 3 and 4.

The input data (of Figs. 1 and 2) consist of the order of $\sim 2^{11}$ data points, the number sufficient to display an exponential scaling but one should have in mind that some statistical errors will be present, as the fractal dimension formula involves the $l \rightarrow 0$ (or, equivalently, the $N \rightarrow \infty$) limit. In fact, for the chaotic case we have got a fairly good scaling in the range of about 8 points in the log-log plot as can be seen from Figs. 3(b). What is important, this scaling persists up to the high q values, *i.e.* to the region where the structure of the probabilities is mostly probed. This kind of scaling has been considerably worsened in the regular case (Fig. 3(a)). In the special case of the capacity dimension we get $D_0 \simeq 1$, as in this case the scaling exponents are determined solely by the energy distribution (see Eq. (2)).

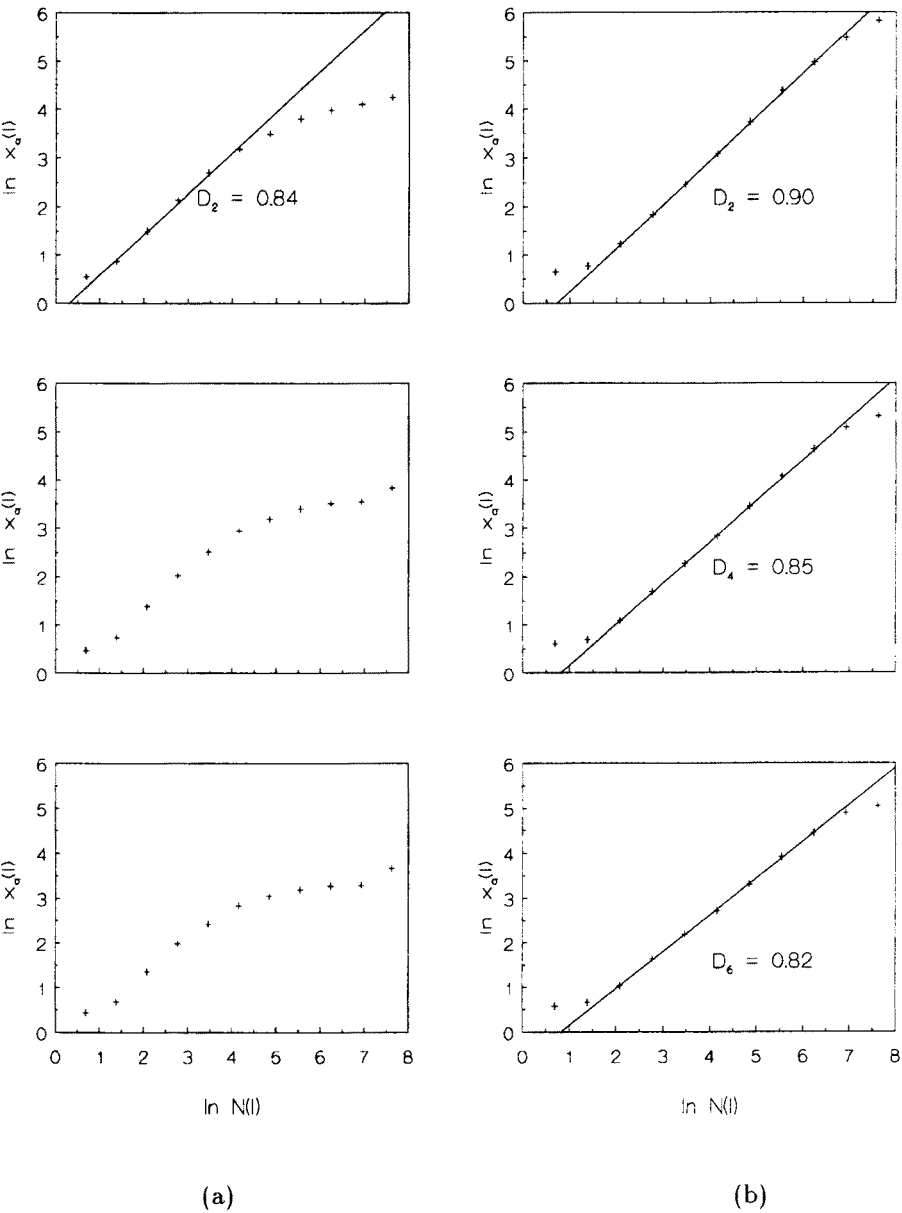


Fig. 3. The log-log plot of $x_q(l)$ of Eq. (14) vs the number of boxes N (equivalent to the inverse of the box size l). $x_q(l)$ is determined by the isovector quadruple transition probabilities in the regular (a) and chaotic (b) case for $q = 2, 4, 6$.

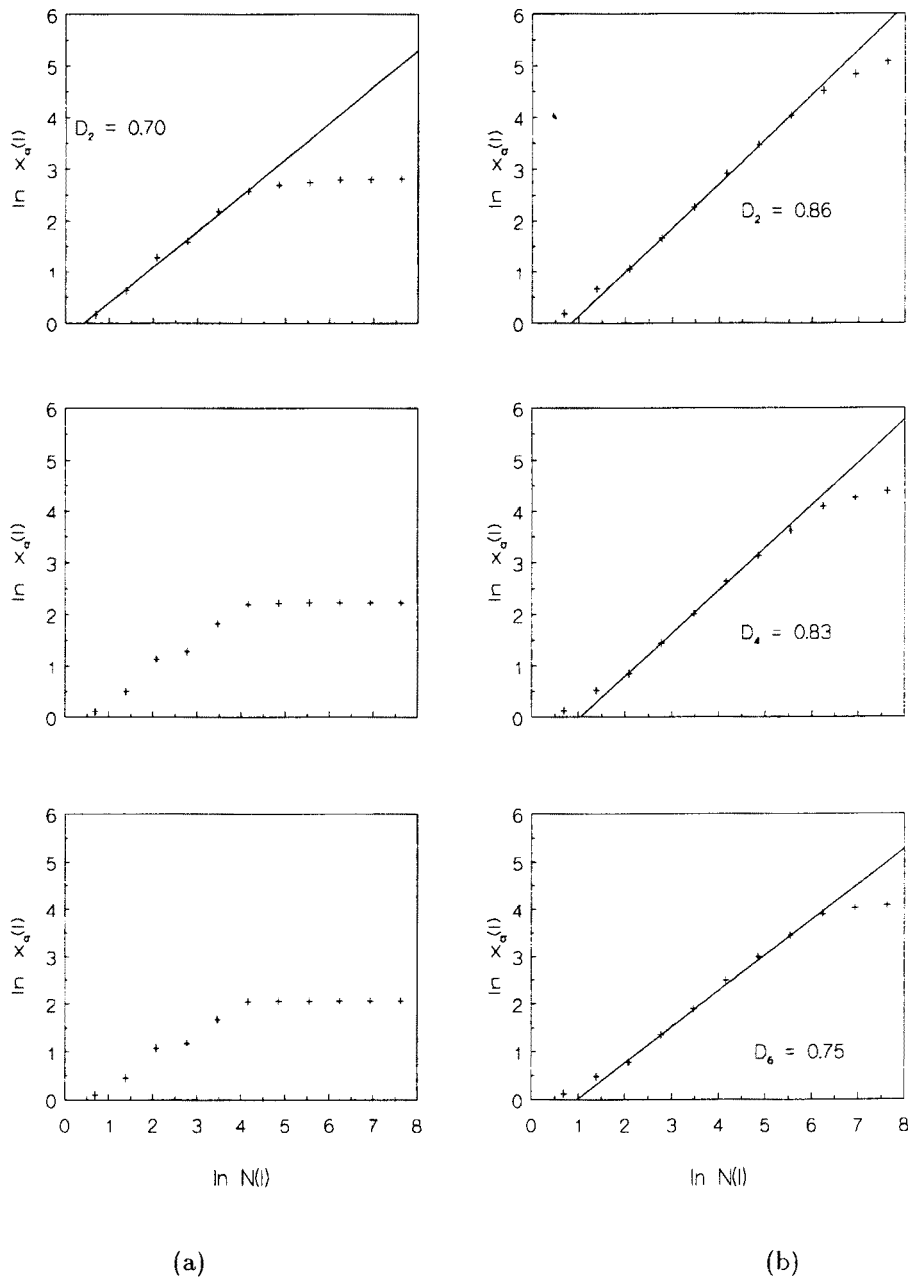


Fig. 4. The same as Fig. 3 for the isoscalar transition probabilities.

This is not a very interesting limit and has not been plotted in Fig. 3(b). The regular case is also plotted for comparison, even though the scaling soon degrades with increasing q and choice of the scaling exponents is difficult in this case. Hence, for $q > 2$ the linear fits have not been plotted in Fig. 3(a). Also, as has been expected, we get larger differences between D_q and $d_q = 1$ for greater q 's.

Analogous plots for the isoscalar transitions are displayed in Fig. 4. One can observe that in this case the scaling exponents (fractal dimensions) are slightly (about 5%) lower which is consistent with the less uniform distribution of the corresponding transition probabilities shown in Fig. 2. Also, the scaling is less evident (its range is shorter, see Fig. 4(b)) even though the fluctuations in the subspace 2 remain the same. This may reflect the fact that the isoscalar giant resonance is more collective¹ than its isovector counterpart and, as such, it is more resistive against decay [14]. In other words, the collectivity is expected to regularize the dynamics and the result seems to confirm such a conjecture.

4. Summary and conclusions

In this paper we have investigated the scaling properties of nuclear giant quadrupole resonance transition probabilities in ^{40}Ca nucleus. These quantities have been computed within the approximation which includes the $1p-1h$ and $2p-2h$ states. The results still preserve the Wigner form of the NNS distribution of energy levels and they are in good agreement with the experimental data (see Figs. 1, 2 and [5, 7]).

To estimate the scaling properties we have introduced a measure defined by (12) which combines the energy spectra and the transition probabilities. This definition allows to make use of the concept of the generalized Renyi exponents [10, 11]. Based on this concept it has been shown that for both, the isovector and the isoscalar transitions, one can speak about the scaling exponents D_q of the multifractal type. This observation applies, however, only to the case when the physics of fragmentation is governed by the chaotic dynamics. These results can be treated as an interesting indication of what are the further signatures of classical chaos on the quantum level.

For the isovector transitions the scaling is somewhat better and the exponents are about 5% higher. This effect may have to do with the fact that the isoscalar resonance is more collective than its isovector counterpart. The collectivity is a natural element regularizing the dynamics.

¹ The notion of the collectivity used here means strong localization of the transition strength in energy and should not be confused for the same notion used in the context of self-organization.

It has been suggested [15] that dynamical systems of the type discussed in this paper can be simulated by the binary, self-similar and conservative random fragmentation process which yields universal behaviour independent of the precise fragmentation mechanism [15, 16]. This gives another justification for neglecting the higher order excitations.

We thank Marek Płoszajczak for very useful discussions. This research was supported by KBN Grant 2 P03B 140 10.

REFERENCES

- [1] M.L. Mehta, *Random Matrices and the Statistical Theory of Energy Levels*, Academic Press, New York 1967.
- [2] O. Bohigas, M.J. Giannoni, C. Schmit, *Phys. Rev. Lett.* **52**, 1 (1984).
- [3] K. Życzkowski, *Acta Phys. Pol.* **B24**, 967 (1993).
- [4] E. Ott, *Chaos in dynamical systems*, Cambridge University Press 1993.
- [5] S. Drożdż, S. Nishizaki, J. Speth, J. Wambach, *Phys. Rev.* **C49**, 867 (1994).
- [6] S. Drożdż, S. Nishizaki, J. Speth, J. Wambach, *Phys. Rep.* **197**, 1 (1990).
- [7] S. Drożdż, S. Nishizaki, J. Wambach, *Phys. Rev. Lett.* **72**, 2839 (1994).
- [8] T.A. Brody, J. Flores, J.B. French, P.A. Mello, A. Pandey, S.S.M. Wong, *Rev. Mod. Phys.* **53**, 385 (1981).
- [9] J.S. Towner, *Phys. Rep.* **155**, 263 (1987).
- [10] J. Balatoni, A. Renyi, *Publ. Math. Inst. Hung. Acad. Sci.* **1**, 9 (1956) [also in: *Selected Papers of A. Renyi*, Vol. 1, Academia Budapest 1976, p. 558].
- [11] G. Paladin, V. Vulpiani, *Phys. Rep.* **156**, 148 (1987).
- [12] T. Geisel, R. Ketzmerick, G. Petschel, *Phys. Rev. Lett.* **66**, 1651 (1991).
- [13] T.C. Halsey, M.H. Jensen, L.P. Kadanoff, I. Procaccia, B.I. Shraiman, *Phys. Rev.* **A33**, 1141 (1986).
- [14] S. Drożdż, S. Nishizaki, J. Wambach, J. Speth, *Phys. Rev. Lett.* **74**, 1075 (1995).
- [15] A.Z. Górski, R. Botet, S. Drożdż, M. Płoszajczak, Proceedings of the 8th Joint EPS-APS International Conference on Physics Computing, September 1996, eds. P. Borchers, M. Bubak, A. Maksymowicz, p. 37-40.
- [16] R. Botet, M. Płoszajczak, *Phys. Rev. Lett.* **69**, 3696 (1992); *J. Mod. Phys.* **E3**, 1033 (1994).